Stability of Graphene Edges under Electron Beam: Equilibrium Energetics *versus* Dynamic Effects

Jani Kotakoski,[†,‡,*] David Santos-Cottin,[†] and Arkady V. Krasheninnikov[†,¶]

[†]Department of Physics, University of Helsinki, P.O. Box 43, 00014 Helsinki, Finland, [‡]Department of Physics, University of Vienna, Boltzmanngasse 5, 1090 Wien, Austria, and [¶]Department of Applied Physics, Aalto University, P.O. Box 1100, 00076 Aalto, Finland

ABSTRACT

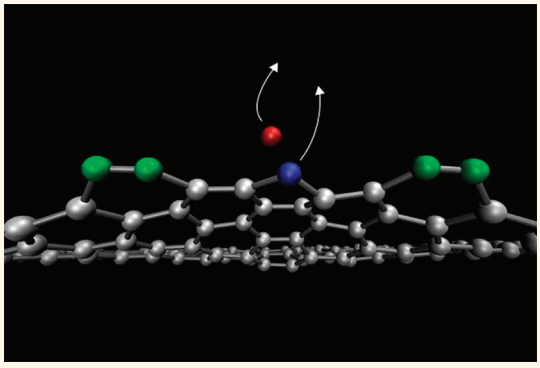

Electron beam of a transmission electron microscope can be used to alter the morphology of graphene nanoribbons and create atomically sharp edges required for applications of graphene in nanoelectronics. Using density-functional-theory-based simulations, we study the radiation hardness of graphene edges and show that the response of the ribbons to irradiation is not determined by the equilibrium energetics as assumed in previous experiments, but by kinetic effects associated with the dynamics of the edge atoms after impacts of energetic electrons. We report an unexpectedly high stability of armchair edges, comparable to that of pristine graphene, and demonstrate that the electron energy should be below ~50 keV to minimize the knock-on damage.

KEYWORDS: graphene · ribbon · edges · electron irradiation · stability

Theoretical predictions[1,2] and subsequent experiments[3,4] demonstrated that a tunable band gap can be opened in graphene—the two-dimensional one-atomic-layer thick carbon membrane[5]—by confining it to a ribbon, thus opening a potential route toward applications of this novel material in nanoelectronics. It occurred, however, that electronic and transport properties of the ribbons are governed by not only ribbon width, but also the morphology of the edges.[6] In fact, controlling the atomic structure of the edges is crucial for any graphene-based electronics. Although many techniques have been suggested for ribbon fabrication and edge manipulation,[7−14] it still remains a challenge to achieve the precision required for a controllable manufacture of atomically sharp edges with a desired crystal orientation.

At the same time, progress in the aberration corrected high resolution transmission electron microscopy (AC-HRTEM) has provided invaluable insights into the atomic structure and properties of graphene sheets and ribbons,[9,15−18] as well as into graphene edge stability and dynamics.[9,14] Moreover, in addition to other irradiation-induced effects,[19,20] it has been demonstrated that the electron beam can also be used for creating nanoribbons and single-atom carbon chains,[7,8] sculpting of predefined graphene-based nanostructures,[14] transforming a graphene flake into a fullerene[21] and layer-by-layer sublimation of graphene.[22,23] Since it was customary to assume that any two-coordinated carbon atom (edge atom) would be equally likely to be removed under an electron beam, the evolution of graphene edges under irradiation was assumed to be governed by equilibrium formation energies of the edges. Similar assumptions have been made for analogous experiments for the structural counterpart of graphene, the *h*-BN monolayer.[24] However, these assumptions completely neglect the dynamic effects of the electron impacts resulting from differences in rigidity of the different edge configurations.

In this study, we employ density-functional-theory (DFT)-based calculations to study the knock-on damage on graphene edges during a TEM experiment. We show that the probability for atom sputtering from the edges is not determined by equilibrium thermodynamics, but by the dynamics of the edge atoms after electron impacts, and that graphene edges with armchair-like reconstructions have the

* Address correspondence to jani.kotakoski@iki.fi.

Received for review October 27, 2011 and accepted December 20, 2011.

Published online December 22, 2011
10.1021/nn204148h

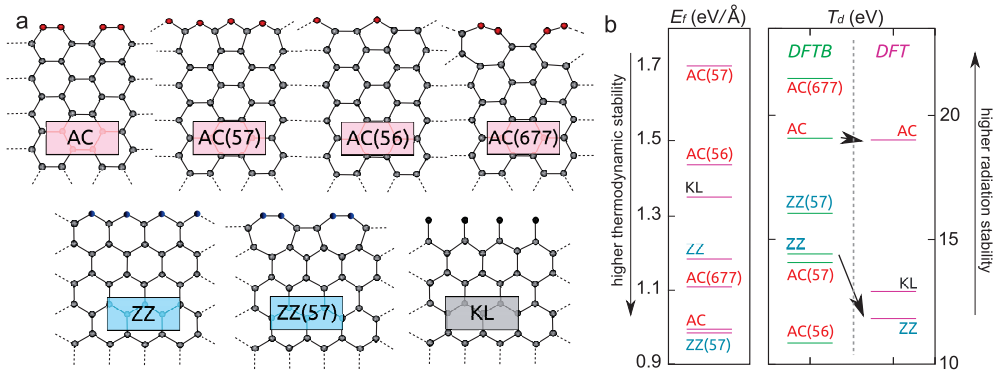

Figure 1. Different edge reconstructions as optimized with DFT (a) and their formation energies E_f and displacement thresholds T_d (b). Displacement thresholds as calculated with both DFT and DFTB are presented. Uncertainties in the T_d are of the order of 0.1 eV.

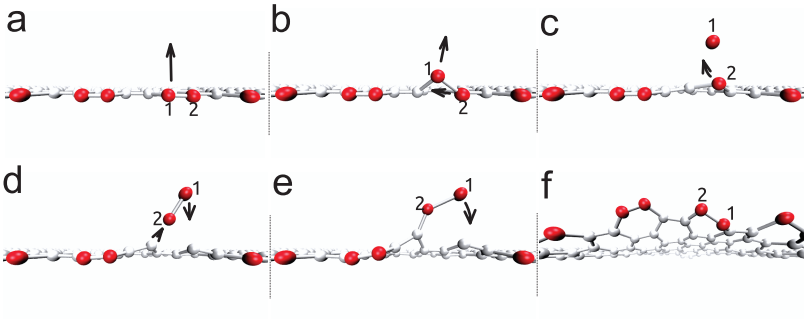

Figure 2. Snapshots of atomic configurations after electron impact onto an AC edge, which did not result in sputtering but gave rise to the *flip* process.

highest radiation stability (almost on par with pristine graphene) which stems from the relatively flexible bonding configuration at the edge. We give new insights into the row-by-row thinning process of graphene nanoribbons under the electron beam, and highlight various edge transformations occurring simply due to the knock-on process. Finally, we demonstrate that the threshold electron energy below which any knock-on damage in graphene should be prevented is ~50 keV, even in defective samples and at the edges. Thus any electron beam damage below this threshold is likely to be due to additional ionization or chemical effects, such as etching due to nonperfect vacuum conditions.

RESULTS AND DISCUSSION

Prior to dynamical simulations of electron impacts onto the edge atoms, we tested our theoretical approach by calculating the edge formation energies ($E_f = [E - N\mu_C]/2l$, where E is the ribbon energy for N atoms and a length of l, and μ_C is the cohesive energy of C in graphene) of different edge configurations (Figure 1) and comparing to the published data.[25−28] Overall, our results proved to be in an excellent agreement with the literature, althought the value we received for the zigzag (ZZ) edge was lower by ~0.1 eV/Å. Also the bond lengths for the optimized structures were in a very good agreement. Upon structure optimization, the Klein (KL) edge reconstructed by forming a bond between the (originally) one-coordinated atoms. We expect this reconstruction to be prevented in the experiments due to hydrogen passivation of the dangling bonds, since the reconstruction does not seem to be present in the experimental images,[29] and therefore used the nonreconstructed geometry for the dynamical calculations.

Next, we moved on to calculations of the minimal kinetic energy trasferred to the nucleus by the impinging electron, which still allows displacing the atom from its lattice position without immediate recombination with the created vacancy, that is, its *displacement threshold* (T_d), for the undercoordinated atoms at armchair (AC), ZZ, and KL edges. The ribbons constructed for this study were assumed to be infinitely long in the x-direction and 6−7 graphene unit cells wide in the y-direction with 7 Å of vacuum introduced between the periodic images of the edges (y-direction) and 15 Å in the z-direction (perpendicular to the ribbon). The DFT-MD results are as follow: $T_d^{AC} \approx 19.0$ eV, $T_d^{ZZ} \approx 12.0$ eV and $T_d^{KL} \approx 12.9$ eV. For comparison, T_d for pristine graphene, calculated with the same method, is $T_d^{GR} \approx 22.0$ eV,[30] whereas the dangling bond atom at a single vacancy has $T_d^{SV} \approx 14.7$ eV and the corresponding atom at a $V_2(5-8-5)$ double vacancy has $T_d^{DV} \approx 16.2$ eV.

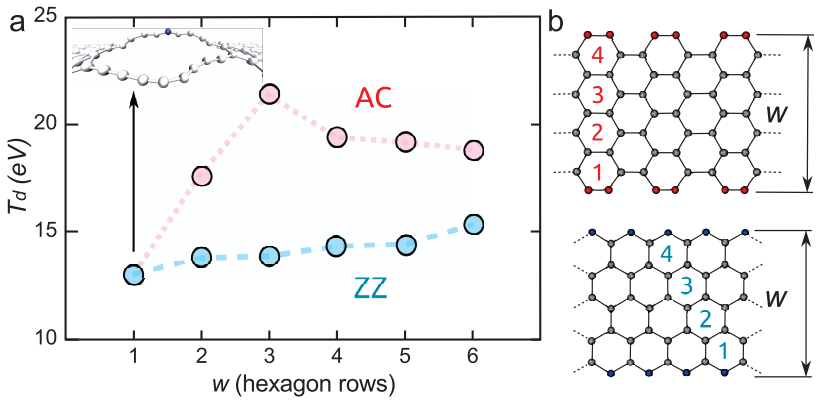

Figure 3. (a) Displacement thresholds T_d of the edge atoms for armchair- (AC) and zigzag-terminated (ZZ) graphene nanoribbons as functions of ribbon width w [as illustrated for the $w = 4$ case in panel b] as calculated with the DFTB method. The inset shows a ZZ-terminated ribbon ($w = 1$) broken into two chains due to an impact on the blue atom.

We checked the effect of hydrogen termination on T_d values, but did not observe significant differences from the nonterminated edges.

From the comparison of the relative order of E_f and T_d for the different edges (Figure 1b), it is immediately evident that radiation stability of the edge cannot be deduced simply from edge formation energy. The observed large differences in T_d for different edges are quite remarkable, since the common practice has been to assume that T_d is roughly equal for any edge atoms. Clearly, our results show that this is not the case. To understand why T_d is different for different two-coordinated atoms, we carefully analyzed time evolution of the atomic structure after several different electron impacts which eventually did not result in sputtering. Simulation snapshots of such a case are presented in Figure 2 for an AC edge. The analysis of atom dynamics indicates that the high T_d^{AC} arises from the fact that the neighboring atom (labeled 2 in Figure 2) follows the displaced atom (labeled 1) at the AC edges, as it is connected to the rest of the system through one bond only. Thus, the kinetic energy provided by the collision is distributed between these two atoms at the early stages after the electron impact. Occasionally this results in a 180° rotation (*flipping*) of the edge dimer, as shown in Figure 2. In the case of KL, the kinetic energy is distributed between the one-coordinated atom and its neighbor on the zigzag edge. This dimer can relatively easily rotate around the edge, which explains the high value of T_d^{KL}. On the other hand, the neighboring atoms at the ZZ edge cannot follow the displaced atom due to the different geometry (two bonds connecting them with the rest of the system). Hence, energy redistribution affects T_d, similar to what has been argued for atoms at vacancy defects in otherwise pristine graphene.[31] The DFTB method seems to overestimate T_d^{ZZ} by ~2.5 eV although T_d^{AC} is very close to the DFT value. We attribute this discrepancy to the differences in the relaxed configurations of the ZZ edge within these two methods: the C−C bonds connecting the ZZ edge to the bulk of the ribbon are elongated by *ca.* 5% when the structure is optimized with DFT, whereas DFTB results only in an elongation of about 2% indicating stronger local bonding. Therefore, during the dynamical DFTB simulations the initial configuration can be further elongated following the displaced atom much more than what is possible during the DFT simulation, which leads to a higher T_d. In the case of an AC edge, both methods lead to smaller changes in the bond lengths close to the edge (~2% for DFT and −1% for DFTB). In addition, the bond which has a stronger effect on the stability of the AC edge is the one between the two atoms of the edge dimer, which is very similar for both methods (~1.23−1.24 Å).

Not only edge morphology, but also the geometry of the larger structure plays a role in the radiation stability. Moreover, experiments have revealed that single-atomic carbon chains derived from nanoribbons are surprisingly stable under the electron beam.[7,8] To study how the T_d of the edge atoms is affected by the ribbon width, we constructed nanoribbons with AC and ZZ edges and widths (w) of one to five rows of hexagons. T_d as a function of w is presented in Figure 3. We first note that T_d increases with w, as the ribbon becomes stiffer. Interestingly, there is a maximum on the curve associated with with unexpectedly high (close to pristine graphene) stability for an AC-terminated ribbon with a width of three hexagon rows. This happens because for $w = 3$ the ribbon is still quite flexible so that the displacement field initiated by the electron impact reaches the other side of the ribbon before the displaced atom leaves the system. Therefore, the kinetic energy is distributed over all atoms, and the whole ribbon can locally follow the displaced atom, making a sputtering event less probable. For $w > 3$, the additional hexagon rows lead to a higher rigidity and thus lower T_d. This does not happen for the overall more rigid ZZ edge. We note that due to overestimated ZZ edge values obtained with the DFTB method,

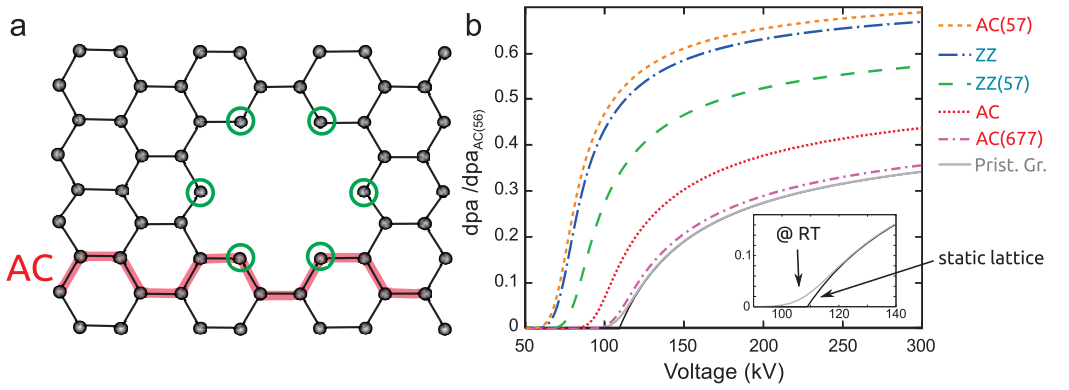

Figure 4. (a) Hole in graphene created by an electron beam, with under-coordinated atoms which are equally likely to be sputtered away marked with circles. Removing any of these atoms results in zigzag edges. (b) Relative displacement rate (displacements per second) for different edge configurations as compared to the least stable one [$dpa_{AC(56)}$ = 1] at room temperature. Inset shows the difference between a static lattice and a lattice at room temperature for pristine graphene.

the actual difference between T_d for the AC and ZZ edges at larger w is expected to be higher than what is seen in Figure 3.

Our simulations also provide insights into the thinning process. The narrowest ribbons are obviously quite unstable under the electron beam (Figure 3). For an AC-terminated ribbon with w = 1, a displacement simply breaks the hexagon-chain. However, for a ribbon with a ZZ edge, the presented value is the kinetic energy needed to separate two carbon chains from each other (see Figure 3, inset). For immediately breaking one of these chains, a much higher energy is needed (~18 eV). Hence, ZZ-terminated ribbons can relatively easily be thinned down to a single carbon chain, but narrow AC-terminated ribbons, when they appear, tend to break rather than separate into atomic chains. This explains why the experimental process[7,8] is possible: creation of atomic chains is likely during continuous electron irradiation since atoms from the ZZ edges are sputtered faster than from the AC edges, and the ZZ-edges tend to separate into chains before breaking.

The radiation stability of the AC edge counters earlier arguments for the higher stability of the ZZ edge under electron beam at 80 kV.[9,14,32] This discrepancy is probably due to the experimental setup: during the irradiation experiment, growth of a rather small hole due to the electron beam is observed, possibly *via* beam-induced chemical etching. Moreover, it is unlikely to obtain an AC edge by randomly removing under-coordinated atoms from the rim of the hole, since before formation of the AC edge they all have an equal probability to be sputtered (see Figure 4a). Therefore, to obtain a conclusive understanding of the relative stability of the different edge configurations, a new experiment designed for exactly this purpose should be carried out. On the other hand, in accordance with our results, long smooth AC edges have been observed to remain stable at voltages of 60−80 kV.[33] Overall, as can be seen from Figure 1b, T_d tends to be lower for any edge with an AC-like reconstruction, when compared to an otherwise similar edge with a more ZZ-like reconstruction. Unexpectedly high radiation stability of a small ribbon with an edge very similar to AC(677) has also been noticed experimentally,[7] again in line with our theoretical results.

During the displacement simulations, we observed several structural transformations at the edges. The ZZ→ZZ(57) transformation has earlier been predicted[25] from edge formation energies. However, since the bond rotation barrier in graphene is 5−10 eV,[34] this is unlikely to happen *via* thermal activation at typical experimental temperatures. However, we observed this transformation *via* the Stone-Wales mechanism due to an electron impact, similar to what happens in pristine graphene.[31] As shown in Figure 1b, this transformation enhances also the radiation resistivity of the edge due to the AC-like edge reconstruction of ZZ(57). However, since the involved bonds become elongated, the stability is less than that of the actual AC edge. We also observed AC↔AC(57) and AC↔AC(677) reconstructions through the same mechanism. Also, AC↔AC(56) transformation occurs locally always upon sputtering.

Finally, in Figure 4b we plot relative displacement rates for different reconstructed edges as calculated with the DFTB method and McKinley-Feshbach approximation,[35] as a function of the TEM acceleration voltage. To take into account the effect lattice vibrations have on the energy transfer,[36] we have assumed Maxwell−Boltzmann distribution for the velocities of the target atoms at room temperature in the direction of the electron beam. As shown in the inset of Figure 4b, this leads to a tail in the collision cross section (and thus displacement rates) toward the lower voltages, but does not significantly change the values above the threshold for the static lattice. We point out that at 80 kV, the knock-on mechanism should be unable to cause sputtering from a static AC edge. At room temperature, the displacement rate approaches

zero below 80 kV, so that the probability for sputtering from the AC edge remains very low at these voltages. In fact, at ~80 kV, an atom from the ZZ edge is ~550 times more likely to be sputtered. However, actual displacement rates remain low enough even for the ZZ edge to allow imaging at normal experimental conditions, and besides, both ZZ and AC edges are subject to chemical etching during AC-HRTEM imaging, which can reduce the observed differences. At 200 kV, the ratio of the displacement rates for these two edges is roughly 5:3. Disregarding the AC(56) reconstruction, which would occur by sputtering a row of atoms from the AC edge, the lowest T_d among all structures is for the AC(57) edge. However, also this edge is much less likely to appear than the AC or ZZ edges due to a high edge energy (Figure 1). Based on our DFT calculations, the acceleration voltage threshold for a stationary ZZ edge is 62 kV (resulting in negligible displacement probabilities at ~50 kV at room temperature).

CONCLUSIONS

In summary, our DFT-based atomistic simulations provide new insights into the development of knock-on damage in graphene edges due to electron irradiation inevitably occurring during imaging in a HRTEM device, and allow more rigorous analysis of the experimental results of the evolution of the edges under the beam. Specifically, we demonstrated an unexpectedly high radiation stability of armchair-like graphene edges and the Klein-edges, and showed that thermodynamic stability is different from radiation stability. Our results provide a limit of ~50 kV for acceleration voltage in order to minimize direct knock-on damage even in the presence of edges or other defects in graphene at room temperature.

METHODS

Displacement Threshold Calculations. In our simulations, we followed a well-established approach repeatedly used[30,31,37−40] to model effects of electron irradiation on solid targets. As energy transfer from the impinging energetic electron to the target nucleus occurs at the zepto (10^{-21}) second time scale,[41] we assumed a direct elastic knock-on collision between the electron and the nucleus, so that the nucleus acquires instantaneously a momentum in a relativistic binary collision. Then we used the molecular dynamics (MD) approach to numerically solve the equations of motion for the target atoms after the impact and found the kinetic energy which allows the displacement of the nucleus from its lattice without immediate recombination with the created vacancy, that is, *displacement threshold* (T_d). This is the only simulation setup which takes into account the energy barrier associated with the sputtering process, while in the static approach T_d is approximated by energy differences between the initial and final structures leading to a considerable underestimate of the barrier, as has been demonstrated earlier.[37]

As analytical potential models for MD are normally fitted to reproduce the equilibrium properties of the material, and thus may not work well for out-of-equilibrium processes, we performed MD simulations using DFT-based methods, as implemented in the VASP simulation package[42,43] with projector augmented wave potentials[44] to describe core electrons, and the generalized gradient approximation[45] for exchange and correlation. For structure optimization and formation energy calculations we used a kinetic energy cutoff for the plane waves of 500 eV. All structures were relaxed until atomic forces were below 0.01 eV/Å. A Monkhorst-Pack **k**-point mesh[46] of 21 × 1 × 1 was used. For dynamical calculations we reduced the cutoff (300 eV) and number of **k**-points (9 × 1 × 1 mesh), as well as increased the system size to avoid interaction between displaced atoms over the cell boundaries. Owing to the high computational cost of DFT-MD simulations, we performed only a few simulations at this level, which served as tests for our simulations using the nonorthogonal DFT-based tight binding (DFTB) method,[47] known to describe reasonably well the energetics of all-carbon structures,[30,31,38,48−50] including displacement threshold for pristine graphene under electron[30] and ion irradiation.[51] All our simulations have been performed on the Born−Oppenheimer potential energy surface, since electronic excitons in such an excellent charge conductor as graphene[6] can be expected to have no contribution to the electron beam damage.

Acknowledgment. We acknowledge support by the Academy of Finland through several projects as well as generous grants of computer time provided by CSC Finland.

REFERENCES AND NOTES

1. Son, Y.-W.; Cohen, M. L.; Louie, S. G. Half-Metallic Graphene Nanoribbons. *Nature* **2006**, *444*, 347–349.
2. Son, Y.-W.; Cohen, M. L.; Louie, S. G. Energy Gaps in Graphene Nanoribbons. *Phys. Rev. Lett.* **2006**, *97*, 216803.
3. Han, M.; Özyilmaz, B.; Zhang, Y.; Kim, P. Energy Band-Gap Engineering of Graphene Nanoribbons. *Phys. Rev. Lett.* **2007**, *98*, 206805.
4. Chen, Z.; Lin, Y.; Rooks, M.; Avouris, P. Graphene Nano-ribbon Electronics. *Phys. E* **2007**, *40*, 228–232.
5. Geim, A. K.; Novoselov, K. S. The Rise of Graphene. *Nat. Mater.* **2007**, *6*, 183–191.
6. Castro Neto, A.; Guinea, F.; Peres, N.; Novoselov, K.; Geim, A. The Electronic Properties of Graphene. *Rev. Mod. Phys.* **2009**, *81*, 109–162.
7. Chuvilin, A.; Meyer, J. C.; Algara-Siller, G.; Kaiser, U. From Graphene Constrictions to Single Carbon Chains. *New J. Phys.* **2009**, *11*, 083019.
8. Jin, C.; Lan, H.; Peng, L.; Suenaga, K.; Iijima, S. Deriving Carbon Atomic Chains from Graphene. *Phys. Rev. Lett.* **2009**, *102*, 205501.
9. Girit, C. O.; Meyer, J. C.; Erni, R.; Rossell, M. D.; Kisielowski, C.; Yang, L.; Park, C.-H.; Crommie, M. F.; Cohen, M. L.; Louie, S. G.; Zettl, A. Graphene at the Edge: Stability and Dynamics. *Science* **2009**, *323*, 1705–1708.
10. Jia, X.; Hofmann, M.; Meunier, V.; Sumpter, B. G.; Campos-Delgado, J.; Romo-Herrera, J. M.; Son, H.; Hsieh, Y.-P.; Reina, A.; Kong, J.; *et al.* Controlled Formation of Sharp Zigzag and Armchair Edges in Graphitic Nanoribbons. *Science* **2009**, *323*, 1701–1705.
11. Jiao, L.; Zhang, L.; Wang, X.; Diankov, G.; Dai, H. Narrow Graphene Nanoribbons from Carbon Nanotubes. *Nature* **2009**, *458*, 877–880.
12. Santos, H.; Chico, L.; Brey, L. Carbon Nanoelectronics: UnzippingTubes into Graphene Ribbons. *Phys. Rev. Lett.* **2009**, *103*, 086801.

13. Cruz-Silva, E.; Botello-Méndez, A.; Barnett, Z.; Jia, X.; Dresselhaus, M.; Terrones, H.; Terrones, M.; Sumpter, B.; Meunier, V. Controlling Edge Morphology in Graphene Layers Using Electron Irradiation: From Sharp Atomic Edges to Coalesced Layers Forming Loops. *Phys. Rev. Lett.* **2010**, *105*, 045501.
14. Song, B.; Schneider, G. F.; Xu, Q.; Pandraud, G.; Dekker, C.; Zandbergen, H. Atomic-Scale Electron-Beam Sculpting of Near-Defect-Free Graphene Nanostructures. *Nano Lett.* **2011**, *11*, 2247–2250.
15. Meyer, J. C.; Kisielowski, C.; Erni, R.; Rossell, M. D.; Crommie, M. F.; Zettl, A. Direct Imaging of Lattice Atoms and Topological Defects in Graphene Membranes. *Nano Lett.* **2008**, *8*, 3582–3586.
16. Gass, M. H.; Bangert, U.; Bleloch, A. L.; Wang, P.; Nair, R. R.; Geim, A. K. Free-Standing Graphene at Atomic Resolution. *Nat. Nanotechnol.* **2008**, *3*, 676–681.
17. Warner, J. H.; Rümmeli, M. H.; Ge, L.; Gemming, T.; Montanari, B.; Harrison, N. M.; Büchner, B.; Briggs, G. A. D. Structural Transformations in Graphene Studied with High Spatial and Temporal Resolution. *Nat. Nanotechnol.* **2009**, *4*, 500–504.
18. Kotakoski, J.; Krasheninnikov, A.; Kaiser, U.; Meyer, J. From Point Defects in Graphene to Two-Dimensional Amorphous Carbon. *Phys. Rev. Lett.* **2011**, *106*, 105505.
19. Krasheninnikov, A. V.; Banhart, F. Engineering of Nanostructured Carbon Materials with Electron or Ion Beams. *Nat. Mater.* **2007**, *6*, 723–733.
20. Krasheninnikov, A. V.; Nordlund, K. Ion and Electron Irradiation-Induced Effects in Nanostructured Materials. *J. Appl. Phys.* **2010**, *107*, 071301.
21. Chuvilin, A.; Kaiser, U.; Bichoutskaia, E.; Besley, N. a.; Khlobystov, A. N. Direct Transformation of Graphene to Fullerene. *Nat. Chem.* **2010**, *2*, 450–453.
22. Huang, J. Y.; Qi, L.; Li, J. *In Situ* Imaging of Layer-By-Layer Sublimation of Suspended Graphene. *Nano Research* **2010**, *3*, 43–50.
23. Dimiev, A.; Kosynkin, D. V.; Sinitskii, A.; Slesarev, A.; Sun, Z.; Tour, J. M. Layer-by-Layer Removal of Graphene for Device Patterning. *Science* **2011**, *331*, 1168–1172.
24. Kim, J. S.; Borisenko, K. B.; Nicolosi, V.; Kirkland, A. I. Controlled Radiation Damage and Edge Structures in Boron Nitride Membranes. *ACS Nano* **2011**, *5*, 3977–3986.
25. Koskinen, P.; Malola, S.; Häkkinen, H. Self-Passivating Edge Reconstructions of Graphene. *Phys. Rev. Lett.* **2008**, *101*, 115502.
26. Okada, S. Energetics of Nanoscale Graphene Ribbons: Edge Geometries and Electronic Structures. *Phys. Rev. B* **2008**, *77*, 041408.
27. Koskinen, P.; Malola, S.; Häkkinen, H. Evidence for Graphene Edges Beyond Zigzag and Armchair. *Phys. Rev. B* **2009**, *80*, 073401.
28. Liu, Y.; Dobrinsky, A.; Yakobson, B. Graphene Edge from Armchair toZigzag: The Origins of Nanotube Chirality? *Phys. Rev. Lett.* **2010**, *105*, 235502.
29. Suenaga, K.; Koshino, M. Atom-by-Atom Spectroscopy at Graphene Edge. *Nature* **2010**, *468*, 1088–1090.
30. Kotakoski, J.; Jin, C.; Lehtinen, O.; Suenaga, K.; Krasheninnikov, A. Electron Knock-On Damage in Hexagonal Boron Nitride Monolayers. *Phys. Rev. B* **2010**, *82*, 113404.
31. Kotakoski, J.; Meyer, J.; Kurasch, S.; Santos-Cottin, D.; Kaiser, U.; Krasheninnikov, A. Stone-Wales−type Transformations in Carbon Nanostructures Driven by Electron Irradiation. *Phys. Rev. B* **2011**, *83*, 245420.
32. Yu, Q.; Jauregui, L. A.; Wu, W.; Colby, R.; Tian, J.; Su, Z.; Cao, H.; Liu, Z.; Pandey, D.; Wei, D.; *et al.* Control and Characterization of Individual Grains and Grain Boundaries in Graphene Grown by Chemical Vapour Deposition. *Nat. Mater.* **2011**, *10*, 443–449.
33. Xie, L.; Wang, H.; Jin, C.; Wang, X.; Jiao, L.; Suenaga, K.; Dai, H. Graphene Nanoribbons from Unzipped Carbon Nanotubes: Atomic Structures, Raman Spectroscopy, and Electrical Properties. *J. Am. Chem. Soc.* **2011**, *133*, 10394–10397.
34. Banhart, F.; Kotakoski, J.; Krasheninnikov, A. V. Structural Defects in Graphene. *ACS Nano* **2011**, *5*, 26–41.
35. McKinley, W.; Feshbach, H. The Coulomb Scattering of Relativistic Electrons by Nuclei. *Phys. Rev.* **1948**, *74*, 1759–1763.
36. Iwata, T.; Nihira, T. Atomic Displacements by Electron Irradiation in Pyrolytic Graphite. *J. Phys. Soc. Jpn.* **1971**, *31*, 1761–1783.
37. Banhart, F.; Li, J.; Krasheninnikov, A. Carbon Nanotubes under Electron Irradiation: Stability of the Tubes and Their Action as Pipes for Atom Transport. *Phys. Rev. B* **2005**, *71*, 241408.
38. Zobelli, A.; Gloter, A.; Ewels, C.; Seifert, G.; Colliex, C. Electron Knock-on Cross Section of Carbon and Boron Nitride Nanotubes. *Phys. Rev. B* **2007**, *75*, 245402.
39. Wang, Z.; Gao, F.; Li, J.; Zu, X.; Weber, W. J. Controlling Electronic Structures by Irradiation in Single-Walled SiC Nanotubes: A First-Principles Molecular Dynamics Study. *Nanotechnology* **2009**, *20*, 075708.
40. Holmström, E.; Toikka, L.; Krasheninnikov, A.; Nordlund, K. Response of Mechanically Strained Nanomaterials to Irradiation: Insight from Atomistic Simulations. *Phys. Rev. B* **2010**, *82*, 045420.
41. Banhart, F. Irradiation Effects in Carbon Nanostructures. *Rep. Prog. Phys.* **1999**, *62*, 1181–1221.
42. Kresse, G.; Furthmüller, J. Efficient Iterative Schemes for *ab Initio* Total-Energy Calculations Using a Plane-Wave Basis Set. *Phys. Rev. B* **1996**, *54*, 11169.
43. Kresse, G.; Furthmüller, J. Efficiency of *ab Initio* Total Energy Calculations for Metals and Semiconductors Using a Plane-Wave Basis Set. *Comput. Mater. Sci.* **1996**, *6*, 15–50.
44. Blöchl, P. E. Projector Augmented-Wave Method. *Phys. Rev. B* **1994**, *50*, 17953–17979.
45. Perdew, J.; Burke, K.; Ernzerhof, M. Generalized Gradient Approximation Made Simple. *Phys. Rev. Lett.* **1996**, *77*, 3865–3868.
46. Monkhorst, H.; Pack, J. Special Points for Brillouin-Zone Integrations. *Phys. Rev. B* **1976**, *13*, 5188–5192.
47. Frauenheim, T.; Seifert, G.; Elstner, M.; Niehaus, T.; Köhler, C.; Amkreutz, M.; Sternberg, M.; Hajnal, Z.; Carlo, A.; Suhai, S. Atomistic Simulations of Complex Materials: Ground-State and Excited-State Properties. *J. Phys. Condens. Matter* **2002**, *14*, 3015.
48. Krasheninnikov, A.; Banhart, F.; Li, J.; Foster, A.; Nieminen, R. Stability of Carbon Nanotubes under Electron Irradiation: Role of Tube Diameter and Chirality. *Phys. Rev. B* **2005**, *72*, 125428.
49. Krasheninnikov, A. V. Predicted Scanning Tunneling Microscopy Images of Carbon Nanotubes with Atomic Vacancies. *Sol. Stat. Commun.* **2001**, *118*, 361–365.
50. Krasheninnikov, A. V.; Nordlund, K.; Foster, A. S.; Ayuela, A.; Nieminen, R. M. Adsorption and Migration of Carbon Adatoms on Zigzag Nanotubes. *Carbon* **2004**, *42*, 1021–1025.
51. Krasheninnikov, A. V.; Miyamoto, Y.; Tománek, D. Role of Electronic Excitations in Ion Collisions with Carbon Nanostructures. *Phys. Rev. Lett.* **2007**, *99*, 016104.